Journal of Statistical Physics, Vol. 87, Nos. 5/6, 1997

There Is More to Be Learned from the Lorentz Model

A. V. Bobylev,[1,2] Frank A. Maaø,[1] Alex Hansen,[1] and E. H. Hauge[1]

Received February 6, 1996; final July 17, 1996

The classical Lorentz model for charged noninteracting point particles in a perpendicular magnetic field is reconsidered in 2D. We show that the standard Boltzmann equation is not valid for this model, even in the Grad limit. We construct a generalized Boltzmann equation which is, and solve the corresponding initial value problem exactly. By an independent calculation, we find the same solution by directly constructing the Green function from the dynamics of the model in the Grad limit. From this solution an expression for the diffusion tensor, valid for arbitrary short-range forces, is derived. For hard disks we calculate the diffusion tensor explicitly. Away from the Grad limit a percolation problem arises. We determine numerically the percolation threshold and the corresponding geometric critical exponents. The numerical evidence strongly suggests that this continuum percolation model is in the universality class of 2D lattice percolation. Although we have explicitly determined a number of limiting properties of the model, several intriguing open problems remain.

KEY WORDS: Kinetic theory; non-Markovian effects; magnetotransport; percolation.

1. INTRODUCTION

It is remarkable that after all these years the classical Lorentz model[1] still has surprises in store. In this simple caricature of reality, a dilute gas of classical point particles moves in a random array of stationary scatterers (see ref. 2 for a simple introduction). The moving particles do not, by decree, interact with each other, so that the problem is reduced to that of

It is with great pleasure we include this paper in the issue honoring Matthieu Ernst, who not only shares our love for kinetic theory, but who also contributed so much to its modern development.

[1] Institutt for fysikk, NTNU, N-7034, Trondheim, Norway.

[2] Permanent address: Keldysh Institute of Applied Mathematics, Russian Academy of Sciences, 125047, Moscow, Russia.

0022-4715/97/0600-1205$12.50/0

a single moving particle interacting with the scatterers through short-range forces. The linear Lorentz–Boltzmann equation for the one-particle distribution is generally assumed to describe the time evolution of the gas, at least in the Grad limit:[3] $n \to \infty$, $a \to 0$, $na^{D-1} = \text{const}$. Here n is the number density of the scatterers with radius a, and D is the dimensionality of space. The last condition ensures that the mean free path is kept constant in the limit, while the dimensionless density tends to zero, $\rho = na^D \to 0$. In fact, under seemingly mild conditions, the Boltzmann equation (BE) has been proven to be exact in the Grad limit (see ref. 4 for a review of rigorous results).

However, in a recent letter[5] we discussed the Lorentz gas of charged particles, screened "electrons" of charge $-e$, *in two spatial dimensions* and under the influence of a perpendicular magnetic field (see Fig. 1). For this case, conventional wisdom is no longer sufficient. Nevertheless, it is possible to construct a generalized Boltzmann equation (GBE) which is exact in the Grad limit. This equation has an interesting non-Markovian structure directly related to the physical mechanism responsible for the breakdown of the standard BE. In spite of the complicated non-Markovian structure of the GBE, the corresponding initial value problem can be solved essentially explicitly. However, this is not the end of the story. The peculiarities of the 2D Lorentz model of classical magnetotransport are not confined to the Grad limit. Backing off from this limit, we identify a percolation problem and study numerically its critical properties close to threshold. The numerical evidence strongly suggests that this continuum

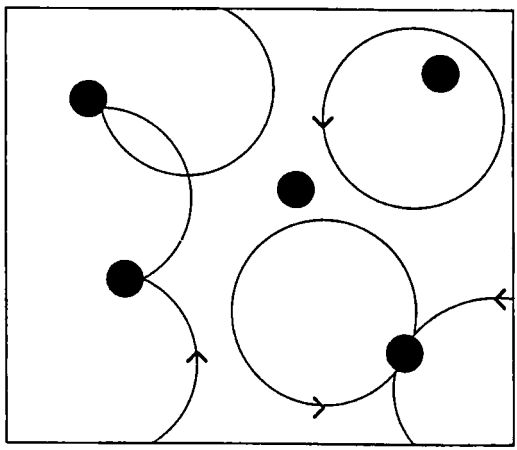

Fig. 1. Typical paths of the moving "electron" (charged particle) in a 2D Lorentz model a perpendicular magnetic field.

percolation model, as far as its equilibrium properties are concerned, is in the same universality class as percolation on a 2D lattice.

In condensed form, we have already presented[5] most of the results to be discussed here. It is the purpose of this paper to provide a fuller view of the problem.

2. THE BOLTZMANN EQUATION

It is useful first to consider the kinetic description provided by the standard Boltzmann equation. For simplicity we restrict ourselves to the spatially homogeneous case, with a one-particle distribution $f(\phi, t)$ depending on time t and on the direction $\phi = \angle(\mathbf{v}, \hat{x})$ of the velocity only. (The speed $v = |\mathbf{v}|$ is a constant of the motion here.) The BE reads

$$\left(\frac{\partial}{\partial t} + \omega \frac{\partial}{\partial \phi}\right) f(\phi, t) = v \int_{-\pi}^{\pi} d\psi \; g(\psi)[f(\phi - \psi, t) - f(\phi, t)] \equiv Bf(\phi, t) \quad (1)$$

The second term on the left describes the action of the magnetic field $\mathscr{B}$, with $\omega = e\mathscr{B}/m$ the cyclotron frequency and m the mass. In the Boltzmann operator B, the collision frequency $\nu = nv\Sigma$ is proportional to the total cross section $\Sigma = \int d\psi \; \sigma(\psi)$, with the dimensionless differential cross section defined as $g(\psi) = \sigma(\psi)/\Sigma$. In classical scattering theory, the total cross section is $\Sigma = 2a$ for *any* 2D interaction potential, nonzero for $r \leqslant a$, and zero otherwise. We restrict ourselves to this class.

The fundamental assumption on which the standard BE is based is the Stosszahlansatz: The moving particle meets every scatterer for the first time; no correlations exist between collisions. It is also taken for granted that there is a constant frequency ν of such collisions. The feature that makes classical magnetotransport in 2D exceptional is that, without scattering, charged particles move in *closed orbits*, in circles with the cyclotron radius $R = v/\omega$. Since the mean free path stays finite in the Grad limit, this implies that there is a finite probability P_0, even in the Grad limit, that an electron will complete an entire cyclotron orbit without scattering. After one revolution without scattering, probability arguments are no longer relevant; it has become *certain* that the electron remains a "circling" electron forever, it will never collide. (An in-plane electric field will destroy this argument!) The existence of circling electrons in the classical 2D Lorentz gas with a perpendicular magnetic field already demonstrates that the standard Boltzmann equation *cannot* be correct in this case. Note that both the dimensionality and the magnetic field are

essential here. With a vanishing magnetic field, the cyclotron radius diverges, and in three spatial dimensions collisionless electrons move in *spirals*, i.e., along trajectories that are not closed.

The physical mechanism that produces the circling electrons is also responsible for a more subtle effect: Recollisions with the same scatterer become possible,[3] even in the Grad limit. After a first encounter with a scatterer, the probability is essentially the same P_0 as above that the electron will be collision-free until it, by the cyclotron orbit, returns to the scatterer with which it already collided. Recollisions flagrantly violate the Stosszahlansatz, and introduce non-Markovian effects into the kinetic theory.

Before we face the task of generalizing the BE, it is necessary to consider the dynamics of collisions and, in particular, of recollision events.

3. THE DYNAMICS OF COLLISIONS

3.1. Single Scattering Events

Consider first a single scattering event, and let the scatterer be a hard disk. Between collisions the electrons move in circular orbits with the radius $R = v/\omega$. Since, with hard disks, the scattering process is completed in a single point, it is unaffected by the magnetic field. Inspection of Fig. 2 shows that the differential cross section is given by

$$\sigma(\psi) = \left|\frac{db}{d\psi}\right| = \left|\frac{d}{d\psi}\left(a \sin\frac{\pi - \psi}{2}\right)\right| = \frac{a}{2}\sin\left|\frac{\psi}{2}\right| \tag{2}$$

or, in dimensionless version, $g(\psi) = \frac{1}{4}\sin|\psi/2|$, since $\Sigma = 2a$. Note that 2D hard disks emphasize backscattering, in contrast to the isotropic scattering from 3D hard spheres.

Clearly the situation is more complicated with soft scatterers, even if the forces vanish beyond the radius a. In this more general case, the motion *during* the scattering process is influenced by the magnetic field. As a result, the differential cross section depends parametrically on the dimensionless ratio a/R. In the Grad limit, however, $a/R \to 0$, and the field dependence of the cross section disappears for any short range scatterer.

[3] Recollisions with large scatterers in a magnetic field have been considered previously on a phenomenological level by several authors. See, in particular, Polyakov.[6]

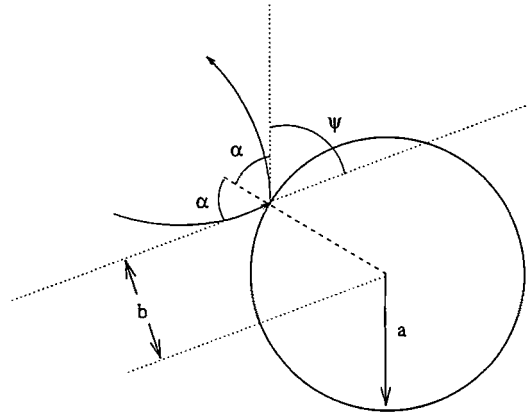

Fig. 2. Scattering off a hard disk of radius a in a magnetic field. The impact parameter is b and the scattering angle is ψ, with $b = a \sin \alpha$ and $\alpha = (\pi - \psi)/2$.

3.2. Repeated Encounters

We return to the hard-disk case and consider the purely dynamical problem of an electron and *a single scatterer*. The electron motion between collisions is all the time along circular orbits, and collisions cause the electron to switch from one cyclotron orbit to the next. That is, as a result of the electron colliding, the *center* of the cyclotron orbit jumps to another position. Figure 3 shows three subsequent collisions with the scatterer. Let the initial cyclotron orbit be no. 1. In the first encounter with the hard disk the electron is scattered over an angle ψ, and switches to cyclotron orbit no. 2. From the symmetry of the event it is clear that cyclotron orbit no. 2 has its center the *same* distance Δ from the center of the scatterer as that of orbit no 1. As a result, orbit no. 2 intersects the scatterer in precisely the same way as orbit no. 1, only shifted an angle 2β along the circumference of the disk. Simple trigonometry shows that β is given by

$$\cos \beta = \frac{\Delta^2 - R^2 + a^2}{2a\Delta} \tag{3}$$

for Δ on the interval $(R-a, R+a)$. That is, in repeated encounters with the hard disk, the scattering angle ψ remains the same, and so does the shift 2β. If β happens to be a rational fraction of 2π, the result is a *periodic trajectory* of finite length. If, on the other hand, Δ is chosen according to a continuous probability distribution, such closed orbits are of measure zero, and we can ignore them. With probability unity the orbits will, in the

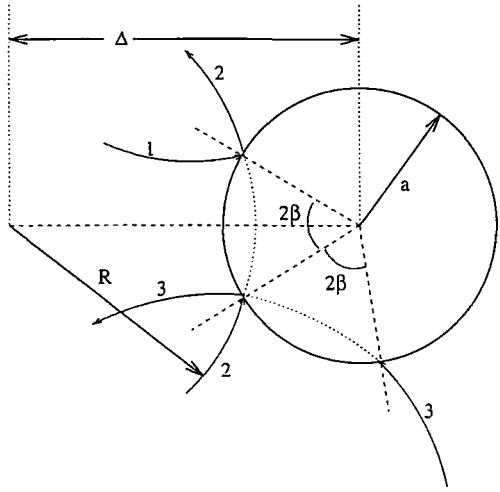

Fig. 3. Successive collisions with a hard-disk scatterer of radius a. Subsequent cyclotron orbits (all with radius R) are numbered 1, 2, and 3. The initial collision makes the electron switch form cyclotron orbit 1 to cyclotron orbit 2, the second from orbit 2 to orbit 3, etc. The distance between the center of a cyclotron orbit and the center of the hard-disk scatterer in Δ. The angle separating two subsequent collision points on the periphery of the disk is 2β.

course of time, densely fill a ring-shaped area around the scatterer, with outer radius $\Delta + R$. With the hard disk replaced by a soft isotropic scatterer, these qualitative conclusions remain unaffected, even though the details of the scattering process become more complicated.

Note that in the Grad limit, where $a/R \to 0$, *two* important simplifications arise: (i) As pointed out above, the differential cross section becomes independent of the magnetic field. (ii) On the length scale set by the size of the scatterer, the cyclotron orbits degenerate into straight lines. This implies that the accumulated scattering angle after s successive encounters with the scatterer equals $s\psi$, where ψ is the scattering angle of the first collision.

4. THE GENERALIZED BOLTZMANN EQUATION

With the dynamics of recollisions with a single scatterer under control, we now return to the Lorentz model in which the number of scatterers is large. One more detail must be cleared up before we can write down the kinetic theory for the model. We need an explicit expression for P_0, the probability that an electron started in a random initial state (but with given v!) completes a cyclotron orbit without suffering collisions. We have

not yet passed to the Grad limit, but we insist that the centers of the scatterers are randomly distributed on the plane with uniform density n (i.e., no correlations between the positions of the scatterers, no penalty for overlaps!). The scatterers, soft or hard, have a radius a. For a point electron to remain unperturbed during an entire revolution in a cyclotron orbit of radius R, the area between the circles with radii $R-a$ and $R+a$ must be free of scattering centers. This area is $A_0=\pi[(R+a)^2-(R-a)^2]=2\pi R\cdot 2a$. The probability that it is free of scattering centers is

$$P_0=\exp(-A_0 n)=\exp(-2\pi R\cdot 2na)\equiv\exp(-2\pi R/\Lambda)$$

The last equality defines our mean free path, $\Lambda=1/(2na)$. As the Grad limit is approached, Λ remains constant. Note that this definition of the mean free path coincides with $\Lambda=1/(n\Sigma)$. Introducing the collision frequency, $\nu=n v\Sigma=2nva$, we can write $P_0=\exp(-\nu T)$, where $T=2\pi/\omega$ is the period in a cyclotron orbit.

The area A that has to be free of scattering centers for a *recollision* to take place is not quite equal to A_0, and Fig. 3 shows that, away from the Grad limit, the precise value of this area depends on the details of the situation: the distance Δ, all previous encounters with the scatterers, etc. However, no detailed calculations are necessary to arrive at the conclusion that the *difference* between A_0 and any particular A of relevance to a recollision event is of $\mathcal{O}(a^2)$. This means that, in the Grad limit, $An\to A_0 n=2\pi R/\Lambda$. As a consequence, in this limit, $P_0=\exp(-2\pi R/\Lambda)=\exp(-\nu T)$ represents *both* the probability of completing a first cyclotron orbit without collisions *and* the probability of returning via such an orbit to a scatterer for an additional encounter. (Here we disregard the possibility of periodic trajectories, of measure zero, as discussed in Section 3.2.)

Since the probability is unity that the electron sweeps out new territory every time it embarks on a cyclotron orbit between successive collisions with a given scatterer, the chance of survival continues to decay exponentially. In the Grad limit, therefore, the probability is unity that the initial state separates the electrons into two, and only two, distinct classes: With probability P_0 the electron is "circling," it never collides with any scatterer. In contrast the probability is $1-P_0$ that it is "wandering" and, in the course of time, will collide with *infinitely* many *different* scatterers. Note that this simple classification only applies in the Grad limit. For finite values of a and n, the options are not only zero and infinity, but the electron can get trapped in clusters of any finite number of scatterers. We shall return to this situation in Section 7.

Let us summarize the simplifying features introduced by passage to the Grad limit:

• Modulo initial states of measure zero, an electron either remains collisionless or it collides, in the course of time, with infinitely many different scatterers.

• The electron can only recollide with a given scatterer if no other scatterer has been hit in the meantime. (This is the simplifying essence of the Grad limit in the standard Boltzmann case, and it remains true here: The probability to return to a scatterer previously encountered, by a *random collision sequence*, tends to zero.)

• The total scattering angle after s successive collisions with the same scatterer is $s\psi$ where ψ is the scattering angle of the first encounter with that scatterer.

Finally, it is important to realize that the initial collision in a recollision series is of standard probabilistic Boltzmann type, whereas the subsequent ones, weighted by powers of P_0, can be described by dynamics alone. This set of properties of the dynamics in the Grad limit of the Lorentz model is sufficient to enable us to directly write down the generalized Boltzmann equation:

$$\left(\frac{\partial}{\partial t}+\omega\frac{\partial}{\partial\phi}\right)f^{\mathrm{G}}(\phi,t)=\sum_{s=0}^{[t/T]}P_0^s\nu\int_{-\pi}^{\pi}d\psi\;g(\psi)[f^{\mathrm{G}}(\phi-(s+1)\psi,t-sT) -f^{\mathrm{G}}(\phi-s\psi,t-sT)] \tag{4}$$

Here $[t/T]$ is the number of cyclotron periods completed at time t. The superscript G on $f^{\mathrm{G}}(\phi,t)$ refers to the following subtlety: During the initial period one has $[t/T]=0$, and the right-hand side (RHS) of the GBE reduces to that of the standard BE. The distinction between circling and wandering electrons has not yet been fully made, and the one-particle distribution is that for *all* electrons: $f^{\mathrm{G}}=f=f^{\mathrm{C}}+f^{\mathrm{W}}$. For $t\geqslant T$, however, the GBE applies *exclusively* to the wandering electrons: $f^{\mathrm{G}}=f^{\mathrm{W}}$. The time evolution of the circling electrons, once they are identified, is trivial. A consequence of this is that the normalization of f^{G} jumps at $t=T$, from 1 to $1-P_0$.

On the basis of the arguments presented, we assert that the generalized Boltzmann equation (4) is *exact* in the Grad limit. This assertion is strengthened by the fact, demonstrated in the next section, that the initial value problem can be solved in two independent ways: (i) via kinetic theory, i.e., on the basis of the GBE, and (ii) directly from the dynamics of the model, in the Grad limit. The results of the two different procedures are in perfect agreement. We are confident that the GBE is indeed exact. Nevertheless, the GBE raises two intriguing problems: How to derive (preferably with leading correction terms) the GBE from the hierarchy,[4]

the royal road to *every* kinetic equation? And, how to construct a mathematically rigorous derivation of the GBE?

5. SOLUTION OF THE INITIAL VALUE PROBLEM

In order to solve the initial value problem posed by the GBE, we first introduce Fourier transforms in angles and Laplace transforms in time,

$$F_m(p) = \int_0^\infty dt\, e^{-pt} f_m(t) = \int_0^\infty dt\, e^{-pt} \int_{-\pi}^{\pi} d\phi\, e^{im\phi} f(\phi, t) \tag{5}$$

The Fourier transform of the right-hand side of the GBE reads, after a change in the order of integrations,

$$\nu \sum_{s=0}^{[t/T]} P_0^s \int_{-\pi}^{\pi} d\psi\, g(\psi)\, e^{ims\psi} (e^{im\psi} - 1)\, f_m^{\mathrm{G}}(t - sT) \tag{6}$$

With $P_0 = e^{-\nu T}$, the Fourier–Laplace transform of the RHS of the GBE reads, after a change in the order of summation over s with integrations over time and scattering angle,

$$\nu \int_{-\pi}^{\pi} d\psi\, g(\psi) \frac{e^{im\psi}}{1 - e^{-(\nu + p)T + im\psi}} F_m^{\mathrm{G}}(p) \tag{7}$$

When one performs the Fourier–Laplace transform of the LHS of the GBE, note must be taken of the sudden change of meaning of $f^{\mathrm{G}}(\phi, t)$ at $t = T$. One finds

$$\begin{aligned} &pF_m^{\mathrm{G}}(p) + [e^{-pt} f_m^{\mathrm{G}}(t)]_0^{T-} + [e^{-pt} f_m^{\mathrm{G}}(t)]_{T+}^{\infty} - im\omega F_m^{\mathrm{G}}(p) \\ &\quad = (p - im\omega)\, F_m^{\mathrm{G}}(p) - (1 - e^{-(p+\nu)T})\, f_m(0) \end{aligned} \tag{8}$$

using the fact that $f_m^{\mathrm{C}}(T) = \exp[-(\nu - im\omega)\, T]\, f_m(0) = e^{-\nu T} f_m(0)$.

The general solution of the initial value problem posed by the GBE is therefore, in Fourier–Laplace form,

$$F_m^{\mathrm{G}}(p) = \frac{(1 - e^{-(p+\nu)T}) f_m(0)}{p - im\omega + \nu \int_{-\pi}^{\pi} d\psi\, g(\psi)(1 - e^{im\psi})/(1 - e^{-(p+\nu)T + im\psi})} \tag{9}$$

This result is valid for *any* interaction of short range. In order to perform the integration over ψ, the differential cross section corresponding to this interaction must be specified.

As announced previously, this is not the only way to solve the initial value problem. Since the dynamics underlying the GBE is well defined, and quite simple in the Grad limit, it is possible to *directly* construct the Fourier–Laplace transform of the Green function

$$F_m(p) = \int_0^\infty dt\, e^{-pt} \int_{-\pi}^{\pi} d\phi\, e^{im\phi} f(\phi, t) \equiv \int_0^\infty dt\, e^{-pt} \langle e^{im\phi(t)} \rangle \tag{10}$$

with $f(\phi, 0) = \delta(\phi)$. Here $\langle \exp[im\phi(t)] \rangle$ is interpreted as an average over the random function $\exp[im\phi(t)]$, with $\phi(0) = 0$. The properties of the random function follow from the dynamics of the model. The calculation is fairly complicated and is consequently relegated to the Appendix. The result is in perfect accord with (9) when note is taken of the fact that $F_m(p)$ includes the circling electrons, also for $t \geqslant T$, whereas $F_m^G(p)$ does not. As a consequence,

$$F_m(p) = F_m^G(p) + \frac{e^{-(p+\nu)T}}{p - im\omega} \tag{11}$$

6. THE DIFFUSION TENSOR

From the Green function (11), i.e., from (9), the diffusion tensor of the Lorentz gas immediately follows. The Einstein–Kubo formula gives, with the understanding that $\phi(0) = 0$,

$$\begin{aligned} D_{xx} = D_{yy} &= \int_0^\infty dt \langle v_x(t)\, v_x(0) \rangle = \tfrac{1}{2} v^2 \int_0^\infty dt \langle \cos \phi(t) \rangle \\ D_{yx} = -D_{xy} &= \int_0^\infty dt \langle v_y(t)\, v_x(0) \rangle = \tfrac{1}{2} v^2 \int_0^\infty dt \langle \sin \phi(t) \rangle \end{aligned} \tag{12}$$

For the asymptotics of the mean square displacement only the symmetric part of the tensor plays a role, and the antisymmetric off-diagonal elements are consequently irrelevant in that context. With an externally imposed gradient, however, the off-diagonal elements acquire physical significance. In fact, even the circling electrons contribute to the off-diagonal elements. It is convenient to introduce the complex diffusion constant $\mathscr{D} = D_1 + iD_2$, with $D_1 = D_{xx}$ and $D_2 = D_{yx}$. Then the Kubo formula acquires the compact form

$$\mathscr{D} = \tfrac{1}{2} v^2 \int_0^\infty \langle e^{i\phi(t)} \rangle_{\phi(0)=0} = \tfrac{1}{2} v^2 F_1(0) \tag{13}$$

From (11) and (9) the diffusion tensor follows as[4]

$$\mathscr{D} = \frac{1}{2} v^2 \left[\frac{e^{-\nu T}}{-i\omega} + \frac{1 - e^{-\nu T}}{\nu \int_{-\pi}^{\pi} d\psi \; g(\psi)(1 - e^{i\psi})/(1 - e^{-\nu T + i\psi}) - i\omega} \right] \tag{14}$$

This result is valid for any interaction of short range.

We now specialize to hard disks by using (2), or its dimensionless Fourier transform, $g_m = -(4m^2 - 1)^{-1}$. Proceeding via infinite series, one can perform the ψ-integration in (14) for this case. The result is

$$\mathscr{D} = \frac{1}{2} v^2 \left[\frac{x^2}{-i\omega} + \frac{\tau_D(x)(1 - x^2)}{1 - i\omega\tau_D(x)} \right]; \qquad x = e^{-\nu T/2} = e^{-\pi\nu/\omega} = e^{-\pi m v/(Ae\mathscr{B})} \tag{15}$$

$$\tau_D^{-1}(x) = \nu \left[1 - \frac{1 - x^2}{2x^2} \left(\frac{1 - x^2}{2x} \ln \frac{1 + x}{1 - x} - 1 \right) \right]$$

The diffusion time scale $\tau_D(x)$ depends only weakly on the magnetic field.[5] As $\mathscr{B} \to 0$, i.e., $x \to 0$, (15) yields $\tau_D^{-1} = (4/3)\,\nu$, in agreement with the result from the standard Boltzmann equation. In the other extreme, $\mathscr{B} \to \infty$, i.e., $x \to 1$, one finds $\tau_D^{-1} = \nu$. (One can understand this physically by noting that, in this limit, the magnetic field acts as an effective randomizer of velocity directions.) There is no interesting structure in τ_D as a function of $\mathscr{B}$ between these extremes. As a result, it is the factor $(1 - x^2) = (1 - e^{-\nu T}) = (1 - P_0)$ that is the most important one. This factor reflects the simple fact that only the wandering electrons (weight $1 - P_0$) contribute to the diffusion process proper. The circling electrons (weight P_0) are trapped in their cyclotron orbits. The qualitative aspects of these results are independent of the details of the interaction.

7. PERCOLATION

We now move away from the Grad limit, keeping both the dimensionless density and the radius of the hard disk relative to the cyclotron radius small, i.e., $\rho = na^2 \equiv (a/l)^2 \ll 1$ and $a/R \ll 1$. Combination of these small quantities gives the new parameter $R/l = R(2\Lambda a)^{-1/2} \equiv r$, of arbitrary magnitude. We note that in the Grad limit, $r \to \infty$. In this limit, the diffusion tensor is given by the GBE, i.e., by (11). On the other hand, for r sufficiently small, no diffusion in the usual sense is possible, since the electrons will, with probability unity, be trapped around a finite cluster of scatterers. As a consequence, there must be a percolation threshold r_p below which the diagonal

[4] The contribution to D_2 from the circling electrons was overlooked in ref. 5.

[5] The small-x expansion of this time is $\tau_D^{-1}(x) = (4/3)\,\nu[1 - x^2/5 - x^4/35 - x^6/105 - \cdots]$. Already the parabolic approximation is reasonable all the way to $x = 1$.

part of the diffusion tensor (defined by taking the macroscopic limit *before* the limit $t \to \infty$ in $\mathscr{D}$) vanishes.

In order to clarify the geometry of this percolation problem, we focus on a scatterer at position $\mathbf{r}_1$. The distance between this scatterer and a scatterer at $\mathbf{r}_i$ is $d_{i1} = |\mathbf{r}_i - \mathbf{r}_1|$. If the cyclotron radius R is less than $\min_{i \neq 1} d_{i1}$, an electron colliding with this scatterer will be trapped around it, eventually sweeping out the area of a circle of radius $2R$ centered at the scatterer. [We have assumed that $a \ll R$, so that corrections to R of $\mathcal{O}(a)$ can be neglected]. Now imagine decreasing the magnetic field, i.e., increasing R until $2R = \min_{i \neq 1} d_{i1}$. The electron will then hit a second scatterer, which we label "2" (so that $d_{21} = \min_{i \neq 1} d_{i1}$). If $d_{21} = \min_{j \neq 1} d_{j1}$, the electron will continue to rescatter only with 1 and 2. These two "active" scatterers define a cluster of size two. However, if $d_{21} > \min_{j \neq 2} d_{j2}$, other scatterers than these two will be hit. When the number of accessible scatterers diverges with the size of the system, there is percolation. The diagonal part of the diffusion tensor no longer vanishes, but becomes finite. The critical cyclotron radius at which this infinite cluster emerges is, by definition, $R_p = r_p l$.

Lorenz *et al.*[7] have studied this percolation problem in a different context. By placing N circles at random inside a unit square and increasing their radii until a path of touching circles appears from one edge of the square to the opposite one, they found[6] $r_p = 0.5993 \pm 0.0007$. Furthermore, they determined the correlation length exponent ν—which in our context is a localization length exponent—to be 1.37 ± 0.07, and the order parameter exponent to be $\beta/\nu = 0.106 \pm 0.003$. The exact results for lattice percolation in two dimensions are[9] $\nu = 4/3$ and $\beta/\nu = 5/48 \approx 0.10417$.

We have studied this percolation problem using an algorithm different from the one sketched above. It is based on the following observation: In Fig. 4 we show two paths $\mathscr{P}$ leading from one edge of the sample to the other. Each path has a critical cyclotron radius $R_c[\mathscr{P}]$ associated with it defined by

$$2R_c[\mathscr{P}] = \max_{(ij) \in \mathscr{P}} d_{ij} \tag{16}$$

If $R \geqslant R_c[\mathscr{P}]$, the electrons may cross the sample by a succession of collisions with the scatterers belonging to $\mathscr{P}$. If $R < R_c[\mathscr{P}]$, this sequence of scatterings is not available. We note, however, that the electrons may still cross the sample through *different* sequences of scatterings involving scatterers belonging to $\mathscr{P}$. Twice the critical radius, which determines whether electrons can move from one edge of the sample to the opposite one, must

[6] An earlier result is that of Shante an Kirkpatrick,[8] who determined the critical volume fraction to be $c_c = 0.68$, corresponding to $r_p = 0.602$.

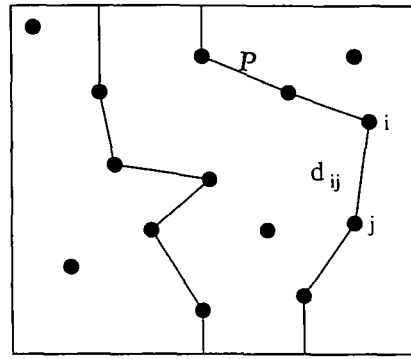

Fig. 4. Two paths $\mathscr{P}$ leading from one edge of the sample to the other. For any of those paths, there is a critical cyclotron radius $2R_c[\mathscr{P}]$ that makes it possible for the electrons to traverse the sample by successively colliding with the scatterers belonging to that path.

be equal to the length d_{ij}^c of the *critical "bond,"* that which minimizes $2R_c[\mathscr{P}]$ over all possible paths $\mathscr{P}$ connecting these two edges,[10]

$$2R_c = d_{ij}^c = \min_{\mathscr{P}} 2R_c[\mathscr{P}] = \min_{\mathscr{P}} \left(\max_{(ij)\in\mathscr{P}} d_{ij} \right) \tag{17}$$

In order to determine R_c for a given sample, we use the following "relaxation" algorithm.[11] Assign to all scatterers a number δ_i, which initially is set equal to the distance from that scatterer to the lower edge of the system. Define a neighborhood $n(i)$ of each scatterer by a set distance Δ chosen so that, on the one hand, $\Delta > 2R_c$, and on the other, Δ is kept small in order to minimize computing time. Go through the list of scatterers and check their neighborhoods $n(i)$ for other scatterers with $\delta_i < \delta_j$. Upgrade the value of δ_i to $\min_{j\in n(i)}[\delta_i, \max(\delta_j, d_{ij})]$. Iterate until convergence. Next consider the horizontal strip S extending Δ down from the upper edge of the system. List the scatterers in this strip, their δ_i, and their distances u_i to the upper edge. For the given sample, a critical percolation path $\mathscr{P}_u^c$ connecting the upper and lower edges of the system is recognized as one which minimizes $\max(\delta_i, u_i)$. There are several such paths, all with the property that they pass through the critical "bond," which determines the critical radius for the sample at hand,

$$2R_c = d_{ij}^c = \min_{i\in S} \max(\delta_i, u_i) \tag{18}$$

The computing time required by this algorithm grows with the system size as $N^{3/2}$, where N is the total number of scatterers.

For a determination of the order parameter exponent, we also need the *size* of the percolation cluster. This is computed as follows: Start with the list of scatterers belonging to one of the critical paths $\mathscr{P}_n^c$. From every scatterer on this path search for scatterers in a neighborhood defined by the distance $2R_c$. Repeat the procedure from every new scatterer found this way. Iterate until all scatterers that can be reached from $\mathscr{P}_n^c$ by steps of lengths not greater than $2R_c$ have been added to the list. Clearly, the end result is independent of which critical path one starts from. The number of scatterers on the list equals, by definition, the size N_c of the critical percolation cluster for the sample at hand. This determination of the critical cluster size does not significantly add to the computing time.

Finally, numbers must be averaged over an ensemble of similar samples. Our numerical results are based on samples containing from $N=312$ to $N=160,000$ scatterers. The number of samples, N_{samp} for each N has been chosen so that $N\times N_{\text{samp}}=2\times 10^6$. In Fig. 5 we show $r_c=R_c/l$ as a function of $N^{-1/2\nu}=N^{-3/8}$. The reason for scaling the abscissa this way is the following: We expect a sample containing N scatterers at its effective percolation threshold to behave like a system with correlation length equal to its linear size $1/l=\sqrt{N}$, in units of l. That is, $|r_p-r_c|^{-\nu}\sim\sqrt{N}$. Solving this equation with respect to r_c, one has

$$r_c=r_p+\frac{A}{N^{1/2\nu}} \tag{19}$$

where A is some constant. However, we see from Fig. 5 that the constant A is very small, and as a consequence, we can only extract the percolation

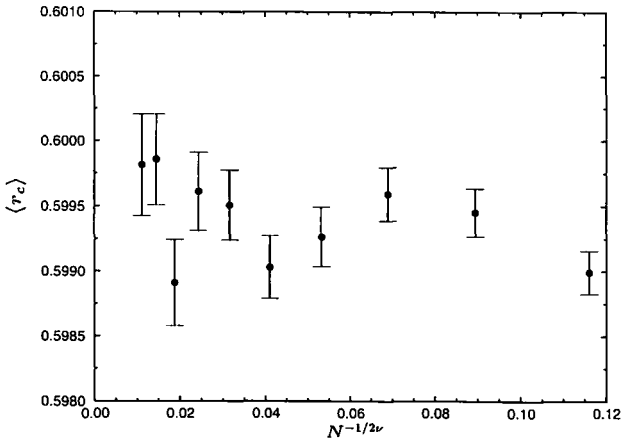

Fig. 5. Effective percolation threshold as a function of $N^{-1/2\nu}$. Extrapolation to $N\to\infty$ gives the percolation threshold. We estimate it to be $r_p=0.5998\pm 0.0005$.

threshold r_p from this figure. Had A been large, only the correct choice for ν would have produced a straight line. We extrapolate r_c for $N \to \infty$ and estimate $r_p = \lim_{N\to\infty} r_c = 0.5998 \pm 0.0005$.

For a determination of the correlation length exponent ν, we record the variance of the effective percolation threshold, $\delta r_c = \sqrt{\langle r_c^2 \rangle - \langle r_c \rangle^2}$ ($\langle \cdots \rangle$ denotes configurational average). From finite-size scaling analysis we expect that

$$\delta r_c \sim N^{-1/2\nu} \tag{20}$$

This quantity is shown in a log–log plot in Fig. 6. Careful inspection of this figure shows that the data points fall on a slightly bent curve, thus indicating important corrections to scaling. In Fig. 7 we show the effective exponent as a function of the smallest N included in the fit. For example, the first data point in this plot gives the exponent as determined from a least squares fit based on all ten data points, while the last data point is based on a least squares fit over the three largest values of N: $N = 40{,}000$, $N = 80{,}000$, and $N = 160{,}000$. It is clear from this figure that the effective exponent is decreasing, and we estimate that $1/2\nu = 0.375 \pm 0.005$. This leads to $\nu = 1.33 \pm 0.02$. Note that the value $\nu = 1.37 \pm 0.07$ reported by Lorenz *et al.*[7] and that found in our previous publication[5] $\nu = 1.37 \pm 0.02$ are mutually consistent. However, the value $\nu = 4/3$, exact for lattice percolation, falls outside the latter estimate. On the basis of our present extensive calculations, we conclude that the discrepancy is due to finite-size corrections. The present data are fully consistent with $\nu = 4/3$ being the exact value also for the Lorentz model.

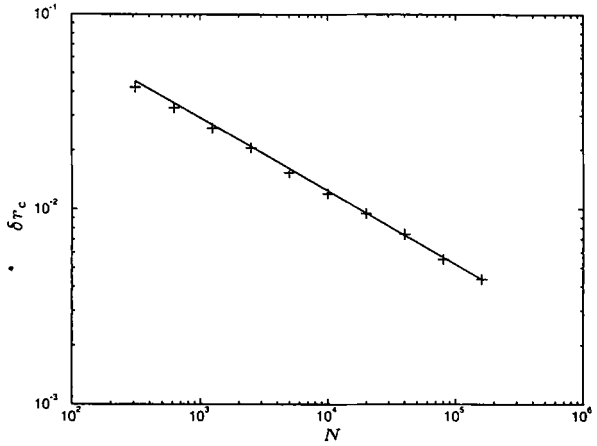

Fig. 6. Variance of r_c as a function of N. The straight line is $AN^{-3/8}$. It acts as a guide to the eye, and indicates that the data points fall on a slightly bent curve.

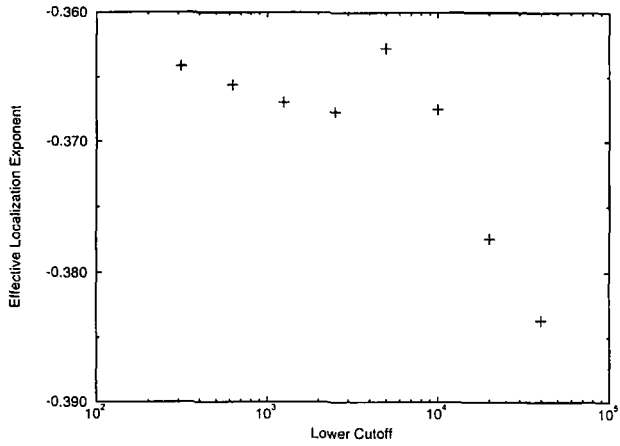

Fig. 7. Effective exponent determined by least-squares fits of the data of Fig. 6 with N larger than some cutoff value recorded along the abscissa. We estimate that $1/2\nu = 0.375 \pm 0.005$.

Finite-size scaling predicts that the fraction of the scatterers that belong to the critical percolation cluster scales like $\langle N_c \rangle / N \sim N^{-\beta/2\nu}$. Our results are shown in Fig. 8. A leastsquares fit of the data gives $\beta/\nu = 0.102 \pm 0.005$, to be compared with the exact value $\beta/\nu = 5/48 \approx 0.104$.

Thus we conclude that all our numerical data are consistent with our model belonging to the same geometric universality class as lattice percolation.

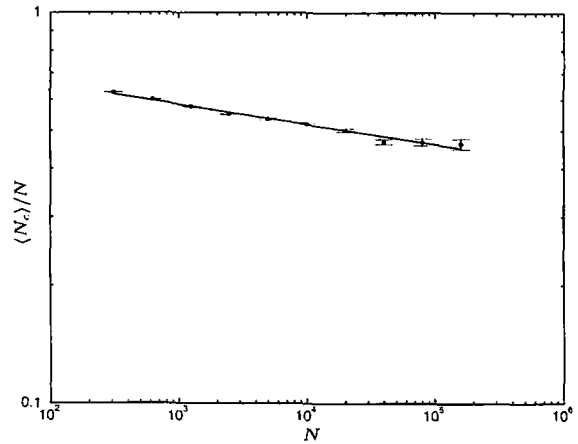

Fig. 8. Relative size of percolating cluster as a function of N. The straight line is a least-squares fit based on all the data points. It has a slope of -0.051.

8. DISCUSSION

8.1. Kinetic Theory

To our knowledge the GBE (4) is the first explicit example of an exact non-Markovian kinetic equation valid for a physical model with well-defined dynamics. Equally important: The initial value problem has been solved exactly in the sense of (9). It is gratifying that the same solution can be found by an independent route, in which one averages over all "paths" from $\phi(0)$ to $\phi(t)$. However, the relative ease by which both methods lead to the solutions is directly related to the simplifications inherent in the Grad limit. We emphasize that a rigorous proof, in the mathematical sense, of the GBE has not been constructed here. The techniques used to establish the Green function directly from the dynamics might be useful in constructing such a proof.

From a physical point of view it seems more important to rederive the GBE from the hierarchy and in the process keep track of the most important correction terms. That this could lead to new insights is emphasized by the fact, explained below, that the Grad limit is in a certain sense singular. We plan to return to a derivation of the GBE from the hierarchy in future work.

The Einstein relation (also its zero-temperature version of relevance in this case) proves, quite generally, that the diffusion and conductivity tensors are proportional to one another. However, introduction of a small but finite electric field $\mathscr{E}$ brings a qualitatively new feature into the problem. In crossed magnetic and electric fields, the center of the cyclotron orbit acquires a drift velocity perpendicular to both and with magnitude $v_d = \mathscr{E}/\mathscr{B}$. As a consequence, the orbits are no longer closed and the mechanism basic to our GBE no longer applies, at least in a strict sense. A rough estimate gives that an electron can recollide with the same scatterer provided that $v_d \lesssim a$. This yields a characteristic value of the electric field, $\mathscr{E}_c = \mathscr{B}a/T = e\mathscr{B}^2 a/(2\pi m)$, beyond which recollisions are no longer relevant. Clearly, $\mathscr{E}_c \to 0$ in the Grad limit, i.e., the diffusion tensor as a function of the electric field becomes singular at $\mathscr{E} = 0$. As the electric field is switched on, $\mathscr{D}$ jumps from the result (15) given by GBE to (presumably) the diffusion tensor which follows from the standard BE. The strongly nonlinear behavior of the conductivity in the small-field region up to $\mathscr{E}_c$ serves as a dramatic illustration of the pitfalls inherent in linear response theory, as pointed out by van Kampen.[12] Furthermore, the above arguments highlight the singular nature of the Grad limit in this model, and demonstrate the importance of studying the leading correction terms away from the limit, *with* a small electric field included (see ref. 20). At this point we note

that if one is sufficiently close to the Grad limit for our result on the diffusion tensor to apply, and the electric field is sufficiently weak that it is meaningful to use the Einstein relation, the magnetoresistence (the difference between the diagonal resistivity and its value at zero magnetic field) is *negative*, and proportional to $x^2 = \exp(-2\pi rmv/(Ae\mathscr{B}))$.

In particular, the open problems indicated above must be clarified before a realistic attempt can be made to relate this model to real physical systems. As is well known, *quantum* magnetotransport in the 2D electron gas has been one of the most active areas of research during the last 15 years (for representative reviews see refs. 13). For a classical description to be realistic, the scatterers must be reasonably large on the scale of the deBroglie wavelength. This points to random arrays of "quantum antidots" as potential candidates. However, the dimensionless density of the scatterers must be small for the GBE to be a good approximation. This raises the problem of ubiquitous disorder potentials, which will act as random electric fields in the plane of the electron gas. In short: The connections, if any, of our model to real physical systems, are yet to be made.

This troublesome perspective shall not deter us from studying this fascinating model for its own sake. We close the discussion on the kinetic theory with three remarks:

- The GBE collision operator is non-Markovian in time, but it is *local* in space. Generalization of the equation to the spatially inhomogeneous case is therefore immediate.

- Ernst and Weijland,[14] 25 years ago, showed that, without a magnetic field, but beyond the Grad limit, the *random* recollisions described by the ring diagrams are reponsible for *algebraic tails* in the velocity autocorrelation function. The recollisions in our case are of a fundamentally different nature, and do not lead to algebraic tails.

- Finally, note that the special role of the magnetic field here is to produce closed orbits. Any other mechanism that produces closed orbits would lead to analogous results. As an artificial example, let the 2D Lorentz gas, *without* a magnetic field, live on the surface of a 3D sphere with a finite radius R: The GBE again applies.

8.2. Percolation

In this paper only the geometric aspects of the percolation problem arising from the Lorentz model have been studied, and the corresponding universality class identified, with reasonable confidence, as that of lattice percolation. Here we add some comments on the *dynamics* close to the percolation threshold.

When the cyclotron radius approaches the critical value $R_c \approx 0.5998l$ from above, we expect diffusion to become anomalously slow. That is, the root-mean-square distance traveled by an electron is expected to grow with time t as t^{1/d_w}, where d_w is known as the random walk dimension.[16] In our model there are two possible sources for this slowing down. One is shared with the lattice percolation problem. Extensive numerical studies of the conductance exponent in lattice percolation[17] has pinned down the value of d_w to $d_w = 2.87$ for that case. The slowing down of lattice percolation can be understood from the topology of the infinite cluster. This cluster is a structure with fractal dimension $2 - \beta/\nu = 91/48 \approx 1.896$, in the shape of a "necklace" of "blobs" (subclusters) joined together by singly connected bonds (i.e., bonds which divide the infinite cluster into two parts if cut). These singly connected bonds themselves form a fractal set of dimension $1/\nu = 3/4$.[18] Bonds in the blobs form two classes: Those belonging to the "backbone" and those belonging to the "dangling ends." The backbone of the infinite cluster is the set of bonds that would carry a current if the infinite cluster were a network of conductors (so that the singly connected bonds also belong to this class). The fractal dimension of the backbone is approximately 1.62.[19] Since this fractal dimension is smaller than that of the infinite cluster itself, it is clear that the dangling ends dominate. Random walkers will get into these dangling ends and spend most of their time looking for the way out of them again. Only when the random walkers move along the backbone do they have a chance of advancing. Furthermore, it is necessary that they find all of the singly connected bonds, a small subset of those belonging to the backbone. These difficulties conspire to change the random walk dimension from 2 to 2.87.

The second possible source for anomalous slowing down of diffusion near the percolation threshold does not exist in the context of lattice percolation, but is specific to Lorentz type models. It is associated with the equivalent of the singly connected bonds: At the percolation threshold, all percolating scattering paths $\mathscr{P}_n^c$ pass through the critical d_{ij}^c defined in Eq. (17). However, there are other d_{ij} through which all percolating paths must pass as well. These are the equivalent of the singly connected bonds in lattice percolation. Let us now focus on the two scatterers defining the critical d_{ij}^c. When the electron scatters on one of them, the next collision will either be with the same scatterer, with the second critical scatterer, or with a third scatterer bringing the electron back into the cluster from which it came. Whenever the electron moves back into the cluster from which it came, it will typically need to reexplore it in full in order to once again find the critical scatterer. This scenario will appear at all the equivalents of the singly connected bonds. If the number of necessary reexplorations before the "singly connected" d_{ij} is crossed has a well-defined average value, the

random walk dimension will be that of lattice percolation. However, there is another possibility: The distribution of necessary reexplorations could fall off by a power law sufficiently slow for such an average not to exist. Should this be the case, the random walk dimension will be larger than that of lattice percolation. We are at present investigating this possibility.

We close by pointing to the following curiosity: For sufficiently *large* dimensionless densities, and with overlapping scatterers, the existence of a percolation threshold based on an entirely different mechanism from the one studied here was pointed out many years ago.[15,2] In the high-density regime the moving particle can simply be trapped in a cage formed by overlapping scatterers. It is therefore a curious fact that with overlapping scatterers and in a magnetic field the diffusive regime as a function of the dimensionless density is bounded by a percolation threshold both from below and from above. Furthermore, with overlapping hard disks the position of the high-density percolation threshold is determined by precisely the same calculation as that reported above. The only difference is that R must now be reinterpreted as the radius a of the overlapping hard disks.

APPENDIX. DIRECT EVALUATION OF THE GREEN FUNCTION

In this Appendix we shall evaluate directly, without reference to the generalized Boltzmann equation, the Fourier–Laplace transform of the Green function (10). The random variables governing $\phi(t)$, and their distribution, are found by direct inspection of the dynamics of the Lorentz gas *in the Grad limit.*

A1. The Random Variables

In the Grad limit, collision sequences in the Lorentz model are of the type

$$122234456788889... \qquad \text{(A1)}$$

In the example shown in (A1), after the collision with scatterer no. 1, the moving particle suffers three consecutive collisions with scatterer no. 2 (as a result of the magnetic field) before it moves on to scatterer no. 3, etc. After the three consecutive collisions with scatterer no. 2, the particle will (with certainty in the Grad limit) never again collide with this particular scatterer. The time of the *initial* collision with scatterer no. i is defined as t_i, and in every collision with this scatterer the angle ψ_i is added to $\phi(t)$. Introducing the time intervals $\tau_i = t_{i-1}$ ($i = 1, 2, 3,...; t_0 \equiv 0$), we identify the following *independent* random variables,

- ψ_i, all distributed on the interval $-\pi < \psi \leqslant \pi$ with a probability density given by the dimensionless cross section $g(\psi)$.

• τ_i $(i=2, 3,...)$, with probability density $p(\tau)=\nu\exp(-\nu\tau)$ on $0\leqslant\tau<\infty$.

• τ_1, with a probability density $p(\tau_1)=\nu\exp(-\nu\tau_1)$ on the interval $0\leqslant\tau_1<T$, integrated to a total weight $1-e^{-\nu T}$, with the remaining weight associated with the probability $P_0=e^{-\nu T}$ that $\tau_1=\infty$, i.e., that no collision takes place.

A2. The Random Function

The random variables defined above completely specify the function $\phi(t\,|\,\tau_1,...;\psi_1,...)$. For convenience from here on we rescale the time variable so that $\nu=1$.

In terms of the reduced angle $\tilde{\phi}(t)=\phi(t)-\omega t$, and with $[x]$ the integer part of x, one has

$$\tilde{\phi}(t_i^-)=\tilde{\phi}(t_{i-1}^-)+(1+[\tau_i/T])\,\psi_{i-1}=\sum_{j=1}^{i-1}(1+[\tau_{j+1}/T])\,\psi_j \tag{A2}$$

Thus, on the interval $t_i<t<t_{i+1}$ $(1\leqslant i<\infty)$ the function $\phi(t\,|\,\tau_1,...;\psi_1,...)$ is specified by the random variables as

$$\phi(t_i<t<t_{i+1})=\sum_{j=1}^{i-1}(1+[\tau_{j+1}/T])\,\psi_j+(1+[(t-t_i)/T])\,\psi_i+\omega t \tag{A3}$$

with the understanding that the sum vanishes for $i<2$. The initial interval $0\leqslant t<t_1$ is special,

$$\phi(0\leqslant t<t_1)=\omega t \tag{A4}$$

However, with the definitions $\psi_0=0$ and $t_0=0$, Eq. (A3) also extends to the case $i=0$.

A3. Summation over Paths in Angle Space

Insertion of (A3) into (10) gives

$$\begin{aligned}F_m(p)&=\left\langle\sum_{k=0}^{\infty}\int_{t_k}^{t_{k+1}}dt\,e^{-pt}e^{im\phi(t)}\right\rangle_{\psi,\tau}\\&=\left\langle\sum_{k=0}^{\infty}\exp\left(\sum_{j=1}^{k}\{-(p-im\omega)\,\tau_j+im(1+[\tau_j/T]\,\psi_{j-1}\}\right)\right.\\&\quad\left.\times\int_0^{\tau_{k+1}}d\tau\exp\{-(p-im\omega)\,\tau+im(1+[\tau/T])\,\psi_k\}\right\rangle_{\psi,\tau}\end{aligned} \tag{A5}$$

where the notation $\langle \cdots \rangle_{\psi,\tau}$ emphasizes that one should average over both the ψ's and the τ's.

Since all the random variables are mutually independent, we can separately average the final τ-integral in (A5) over τ_{k+1}, with the restriction that $k \geqslant 1$:

$$A_k \equiv \left\langle \int_0^{\tau_{k+1}} d\tau \exp\{\cdots\} \right\rangle_{\tau_{k+1}} = \int_0^{\infty} d\tau \exp\{\cdots\} \int_{\tau}^{\infty} d\tau_{k+1} e^{-\tau_{k+1}}$$

$$= \int_0^{\infty} d\tau \exp\{-(p+1-im\omega)\tau + im(1+[\tau/T])\psi_k\}$$

$$= \frac{1-e^{-(p+1)T}}{p+1-im\omega} \frac{e^{im\psi_k}}{1-e^{-(p+1)T+im\psi_k}} \tag{A6}$$

The case $k=0$ requires special treatment, since the probability distribution over τ_1 is special (note that $\psi_0 = 0$),

$$A_0 = \left\langle \int_0^{\tau_1} d\tau\, e^{-(p-im\omega)\tau} \right\rangle_{\tau_1}$$

$$= \int_0^{T} d\tau_1\, e^{-\tau_1} \int_0^{\tau_1} d\tau\, e^{-(p-im\omega)\tau} + e^{-T} \int_0^{\infty} d\tau\, e^{-(p-im\omega)\tau}$$

$$= \frac{e^{-(p+1)T}}{p-im\omega} + \frac{1-e^{-(p+1)T}}{p+1-im\omega} \tag{A7}$$

Now, comparison between (A5) and the second line of (A6) shows that $F_m(p)$ can be written

$$F_m(p) = A_0 + \tilde{A}_0 \left\langle \sum_{k=1}^{\infty} \prod_{j=1}^{k} A_j \right\rangle_{\psi} \tag{A8}$$

with

$$\tilde{A}_0 = \int_0^{T} d\tau_1\, e^{-\tau_1} e^{-(p-im\omega)\tau_1} = \frac{1-e^{-(p+1)T}}{p+1-im\omega} \tag{A9}$$

Since the ψ_i are independent random variables and $\langle A_1 \rangle_{\psi_1} = \langle A_2 \rangle_{\psi_2} = \cdots = \langle A \rangle$, Eq. (A8) simplifies to

$$F_m(p) = A_0 - \tilde{A}_0 + \tilde{A}_0 \sum_{k=0}^{\infty} \langle A \rangle^k = A_0 - \tilde{A}_0 + \frac{\tilde{A}_0}{1-\langle A \rangle} \tag{A10}$$

Finally insert (A7), (A9), and (A6) into (A10), use the fact that $g(\psi)$ integrates to unity, and return to unscaled variables to get

$$F_m(p) = \frac{e^{-(p+\nu)T}}{p - im\omega} + \frac{1 - e^{-(p+\nu)T}}{p - im\omega + \nu \int_{-\pi}^{\pi} d\psi\, g(\psi)(1 - e^{im\psi})/(1 - e^{-(p+\nu)T + im\psi})} \quad \text{(A11)}$$

The first term in Eq. (A11) ($= A_0 - \tilde{A}_0$) is recognized as the contribution to $F_m(p)$ from integrating the circling electrons from $t = T$ to $t = \infty$. This implies that the second term in Eq. (A11), by definition, is identified as $F_m^G(p)$. Comparison with (9) shows that "summation over paths in angle space" gives precisely the same result as the one obtained from the generalized Boltzmann equation.

ACKNOWLEDGMENTS

We thank J. Piasecki for pertinent remarks. A.V.B. is grateful for financial support from The Research Council of Norway, and from grant 93-01-01689 of the Basic Research Foundation of Russia. This work has also received support from The Research Council of Norway (Program for Supercomputing time) for a grant of computing time.

REFERENCES

1. H. A. Lorentz, *Arch. Néerl.* **10**:336 (1905).
2. E. H. Hauge, What can one learn from the Lorentz model? in *Transport Phenomena*, G. Kirczenow and J. Marro, eds. (Springer-Verlag, Berlin, 1974).
3. H. Grad, Principles of the kinetic theory of gases, in *Handbuch der Physik*, Vol. 12, S. Flügge, ed. (Springer-Verlag, Berlin, 1958).
4. H. Spohn, *Rev. Mod. Phys.* **53**:569 (1980); H. Spohn, *Large Scale Dynamics of Interacting Particles* (Springer-Verlag, Berlin, 1991).
5. A. V. Bobylev, F. A. Maaø, A. Hansen, and E. H. Hauge, *Phys. Rev. Lett.* **75**:197 (1995).
6. D. Polyakov, *Zh. Eksp. Teor. Fiz.* **90**:546 (1986) [*Sov. Phys. JETP* **63**:317 (1986)].
7. B. Lorenz, I. Orgzall, and H. -O. Heuer, *J. Phys. A* **26**:4711 (1993).
8. V. K. S. Shante and S. Kirkpatrick, *Adv. Phys.* **20**:325 (1971).
9. M. den Nijs, *J. Phys. A* **12**:1857 (1979).
10. S. Roux, A. Hansen, and E. Guyon, *J. Phys.* (Paris), **48**:2125 (1987); A. Hansen and S. Roux, *J. Phys. A* **20**:L873 (1987).
11. A. Hansen and E. L. Hinrichsen, *Phys. Scripta* **T44**:55 (1992).
12. N. G. van Kampen, *Phys. Norveg.* **5**:279 (1971).
13. R. E. Prange and S. M. Girvin, eds., *The Quantum Hall Effect*, (Springer-Verlag, New York, 1987); C. W. J. Beenakker and H. van Houten, in *Solid State Physics: Advances in Research and Applications*, Vol. 44, H. Ehrenreich and D. Turnbull, eds. (Academic Press, Boston 1991).

14. M. H. Ernst and A. Weijland, *Phys. Lett. A* **34**:29 (1971).
15. E. H. Hauge and E. G. D. Cohen, *J. Math. Phys.* **10**:397 (1969).
16. Y. Gefen, A. Aharony, and S. Alexander, *Phys. Rev. Lett.* **50**:77 (1983).
17. J. M. Normand, H. J. Herrmann, and M. Hajjar, *J. Stat. Phys.* **52**:441 (1988).
18. A. Coniglio, *J. Phys. A* **15**:3829 (1982).
19. H. J. Herrmann and H. E. Stanley, *Phys. Rev. Lett.* **53**:1121 (1984).
20. J. Piasecki, A. Hansen and E. H. Hauge, *J. Phys. A* **30**:795 (1997).